JOURNAL OF VIROLOGY, Apr. 1987 p. 1007–1018
0022-538X/87/041007-12$02.00/0

Vol. 61, No. 4

Alterations in Nuclear Matrix Structure after Adenovirus Infection

ZHAI ZHONGHE,† JEFFREY A. NICKERSON, GABRIELA KROCHMALNIC, AND SHELDON PENMAN*
Department of Biology, Massachusetts Institute of Technology, Cambridge, Massachusetts 02139

Received 3 October 1986/Accepted 2 December 1986

Infection of HeLa cells with adenovirus serotype 2 causes rearrangements in nuclear matrix morphology which can best be seen by gentle cell extraction and embedment-free section electron microscopy. We used these techniques to examine the nuclear matrices and cytoskeletons of cells at 6, 13, 28, and 44 h after infection. As infection progressed, chromatin condensed onto the nucleoli and the nuclear lamina. Virus-related inclusions appeared in the nucleus, where they partitioned with the nuclear matrix. These virus centers consisted of at least three distinguishable areas: amorphously dense regions, granular regions whose granulations appeared to be viral capsids, and filaments connecting these regions to each other and to the nuclear lamina. The filaments became decorated with viral capsids of two different densities, which may be empty capsid shells and capsids with DNA-protein cores. The interaction of some capsids with the filaments persisted even after lysis of the cell. We propose that granulated virus-related structures are sites of capsid assembly and storage and that the filaments may be involved in the transport of capsids and capsid intermediates. The nuclear lamina became increasingly crenated after infection, with some extensions appearing to bud off and form blebs of nuclear material in the cytoplasm. The perinuclear cytoskeleton became rearranged after infection, forming a corona of decreased filament number around the nucleus. In summary, we propose that adenovirus rearranges the nuclear matrix and cytoskeleton to support its own replication.

Adenoviruses are nonenveloped DNA viruses of 70 to 80 nm in diameter (18, 29). After infection, adenovirus virions are transported into the nuclei of host cells, where viral transcription, DNA replication, and virus assembly occur (30). The assembly of virions in the nucleus is not completely understood, but a consensus about the major events in assembly has emerged (19). Virion protein synthesis is detectable by 7 h after infection (42). Capsomeres are assembled in the cytoplasm within minutes after their constituent proteins are synthesized and are quickly transported into the nucleus (20). The capsomeres begin to appear in the nucleus within 15 min of their assembly in the cytoplasm (20). Once in the nucleus, the capsomeres assemble into empty virion shells, lacking DNA and the core proteins. Only later are DNA and the core proteins packaged into these shells (11, 12, 31). This view of adenovirus assembly is based on experiments involving the isolation of such virion shells lacking DNA.

Following adenovirus infection, there are changes in cell morphology which are observable by light microscopy and are referred to as the cytopathic effect (28, 37). Infected cells become more rounded and detach from the culture dish. These gross morphological changes reflect underlying changes in cytoskeletal and nuclear morphology, which are best seen by electron microscopy.

Nuclei contain a highly ordered structure composed of protein and RNA and referred to as the nuclear matrix. This structure has been isolated by a variety of techniques (3–5, 8, 15, 16, 25) and is involved in cell DNA replication (5, 24, 26) and the transcription of active genes (10, 17, 34, 35, 38). Adenovirus DNA is quantitatively bound to the HeLa cell nuclear matrix at 4 to 24 h after infection (39, 44). Adenovirus RNA transcription and pre-mRNA processing are quantitatively associated with the infected-cell nuclear matrix (23). Newly transcribed RNA and the splicing intermediates for adenovirus virion protein L3 and L4 RNAs are associated with the matrix of HeLa cells at 18 h after infection. Several adenovirus early-region proteins become bound to the nuclear matrix, including the E1a positive-acting transcription factors (13, 36). These associations between adenovirus metabolism and the host cell nuclear matrix suggest that adenovirus DNA replication and virion assembly, as well as viral RNA synthesis, might be localized on the nuclear matrix of the infected cell.

The association of adenovirus assembly with the nuclear matrix is not easily seen in ultrastructural studies of infected cells (21, 30). Such studies have involved the use of conventional embedded-section electron microscopic techniques, which cannot image most elements of the nuclear matrix structure (7, 15, 43). In this paper, we report the use of gentle cell extraction techniques and embedment-free section electron microscopy, techniques applied in this laboratory to the study of cell ultrastructure (7, 15), to examine the association of virus metabolism and virion assembly with the nuclear matrix. We show that adenovirus infection causes a major rearrangement of the nuclear matrix and propose that the resulting, altered matrix provides a structural framework on which viral assembly can occur.

MATERIALS AND METHODS

Cell culture and virus infection. Adenovirus serotype 2 was a gift of P. Sharp, Massachusetts Institute of Technology, and was propagated in HeLa S3 cells grown by suspension culture in Eagle minimal essential medium supplemented with 10% fetal bovine or horse serum. HeLa cells (2×10^7 to 4×10^7) were infected synchronously with 20 to 50 PFU (0.5 to 1 50% tissue culture infective dose) of adenovirus per cell in 1 to 2 ml of serum-free medium at 32 to 35°C for 60 min. After infection, the cells were diluted to a volume of 50 to 100 ml with medium supplemented with 5% serum. Control cells were mock infected by the same protocol. Viral titers were determined by the plaque assays of Precious and Russell (32).

* Corresponding author.
† Present address: Department of Biology, Peking University, Beijing, People's Republic of China.

Cell fractionation and electron microscopy. Unless otherwise noted, all fractionation steps were done at 4°C and are essentially as described by Fey et al. (15). Cells were washed with phosphate-buffered saline. For electron microscopy, cell pellets were suspended in cytoskeleton (CSK) buffer, which contains [piperazine-*N*,*N*′-bis(2-ethanesulfonic acid); 10 mM PIPES pH 6.8], 100 mM KCl, 300 mM sucrose, 3 mM $MgCl_2$, 1 mM EGTA, 4 mM vanadyl adenosine, 1.2 mM phenylmethylsulfonyl fluoride, and 0.5% (vol/vol) Triton X-100. After 3 min, the HeLa cytoskeletal frameworks were separated from soluble proteins by centrifugation at 600 × *g* for 3 min. The cytoskeletal framework pellet was extracted in RSB-Magik (42.5 mM Tris hydrochloride [pH 8.3], 8.5 mM NaCl, 2.6 mM $MgCl_2$, 4 mM vanadyl adenosine, 1.2 mM phenylmethylsulfonyl fluoride, 1% [vol/vol] Tween 40, 0.5% [vol/vol] sodium desoxycholate) for 5 min and pelleted as before. This step strips away the cytoskeleton, leaving in the pellet nuclei with their attached intermediate filaments (15). This nuclear pellet was suspended in digestion buffer (CSK buffer except with 50 mM NaCl instead of KCl). RNase-free DNase I (EC 3.1.21.1; Worthington Diagnostics, Freehold, N.J.) which had been purified by the method of Wilchek and Gorecki (41) was added to a final concentration of 200 μg/ml. DNase I digestion proceeded for 20 min at room temperature before ammonium sulfate was added to a final concentration of 0.25 M, and the mixture was incubated for a further 5 min before being pelleted as before. This step in the fractionation removes the chromatin fraction, leaving in the pellets the nuclear matrix-intermediate filament structures containing nuclear ribonucleoprotein (RNP) complexes.

Cells at different stages of fractionation were fixed and prepared for electron microscopy as described by Fey et al. (15). Briefly, samples were fixed in 2.5% (vol/vol) glutaraldehyde in CSK or digestion buffer for 30 min at 4°C, postfixed in 1% (wt/vol) OsO_4 in 0.1M sodium cacodylate (pH 7.2) for 5 min at 4°C, dehydrated in ethanol, and transferred to *n*-butanol before embedment in diethylene glycol distearate. Thin sections were cut by using a Sorvall Porter-Blum MT-2B ultramicrotome with glass knives. The embedding medium was removed in *n*-butanol. Sections were immersed in ethanol, dried through the CO_2 critical point, and examined with a JEOL EM 100 B electron microscope at 80 kV.

Samples to be embedded in Epon were fixed, postfixed, and dehydrated in the same way. The transitional solvent was propylene oxide, and the sample was embedded in Epon-Araldite at 60°C for 2 days. Thin sections were cut as before and double stained with uranyl acetate followed by lead citrate (33).

RESULTS

The organization of adenovirus into virus-specific organizing centers in the infected cell nucleus can be observed in conventional Epon section electron microscopy (21, 30). Observed in this way (Fig. 1a and 1c), HeLa cell nuclei after 28 h of infection contained virus-specific structures, but the fine structure of these viral centers was largely hidden by the embedding resin and by the surrounding cell constituents. The use of such conventional Epon-embedded thin sections has been useful, showing that adenovirus rearranges the nuclear interior, but lack of resolution makes this technique less appropriate for studying virus-caused rearrangements of the nuclear matrix. Selective cell extraction and embedment-free section electron microscopic techniques have been developed in this laboratory and have proved ideal for the detailed examination of the nuclear matrix (7, 15). These new extraction and embedment-free section techniques yield a dramatically enhanced, although complementary, view of the virus-infected nucleus. Throughout this paper, we will examine two different preparations of extracted HeLa cells: cytoskeletal preparations, which are cells extracted with 0.5% Triton X-100, and the RNP-containing nuclear matrix preparations which have been further treated with DNase I and moderate salt concentrations, treatments which remove chromatin but not the nuclear matrix-associated RNP particles.

We could see the ultrastructure of adenovirus-organizing centers in the 28-h-infected HeLa cell nucleus in much better detail in embedment-free sections than in Epon-sections (Fig. 1). In these micrographs, of both cytoskeletal preparations (Fig. 1b) and RNP-containing nuclear matrix preparations (Fig. 1d), large, DNase I-resistant, electron-dense structures were enmeshed in the nuclear matrix and were associated with nuclear matrix filaments that were themselves decorated with viral capsids of about 75 nm in diameter. The nuclear matrix filaments anchored these structures to the nuclear lamina. The electron-dense virus structures had the appearance of altered nucleoli, and, as we shall discuss later, virus-organizing structures may orient themselves around existing nucleoli. In Epon sections (Fig. 1a and c), much of the fine structure of the DNase I-resistant virus centers could not be seen. The filaments of the nuclear matrix were rarely seen in such embedded sections, except in cross-section, so that the spatial relationships between the nuclear matrix filaments and viral capsids and between the filaments and virus-related nuclear structures could not be easily seen.

Figure 2 shows mock-infected HeLa cells that were visualized by our extraction and embedment-free section techniques. As discussed in more detail by Fey et al. (15), the HeLa cell nuclear matrix is a three-dimensional network of filaments bounded by the nuclear lamina. Large electron-dense and DNase I-resistant nucleoli are enmeshed in the interior matrix fibers. After removal of chromatin by DNase I digestion (Fig. 2b), clusters of 25- to 30-nm RNP granules were seen associated with the filaments and could be largely removed by a subsequent RNase digestion (15). Fibers of 10 nm radiated from the exterior of the nuclear lamina into the cytoplasm and were shown to be intermediate filaments tightly associated with the nuclear matrix in a nuclear matrix-intermediate filament complex (15).

We examined the morphological changes in HeLa cells through various stages of adenovirus infection. These images are shown in Fig. 3 and should be compared with the mock-infected controls shown in Fig. 2. It is clear from these pictures that the major effects of adenovirus infection on cell structure are changes in the nuclear matrix. The cytoskeleton was altered but less profoundly than the matrix.

After 6 h of infection (Fig. 3a and b), most nuclei had moved to the periphery of the cell. Such peripheral nuclei were occasionally seen in control cells but were much more common after infection. Chromatin had condensed around the nuclear lamina and around the nucleoli. After treatment with DNase I (Fig. 3b), some nucleoli were vesiculated with a small electron-transparent region in the center. Some filaments of the nuclear matrix were visible. These are 0.1 μm sections through the nuclei (10 μm in diameter), and so only a small fraction of nuclear matrix fibers are visible, but comparisons with control nuclei showed fewer filaments and some that had collapsed onto the nuclear lamina.

By 13 h after infection (Fig. 3c and d), there were

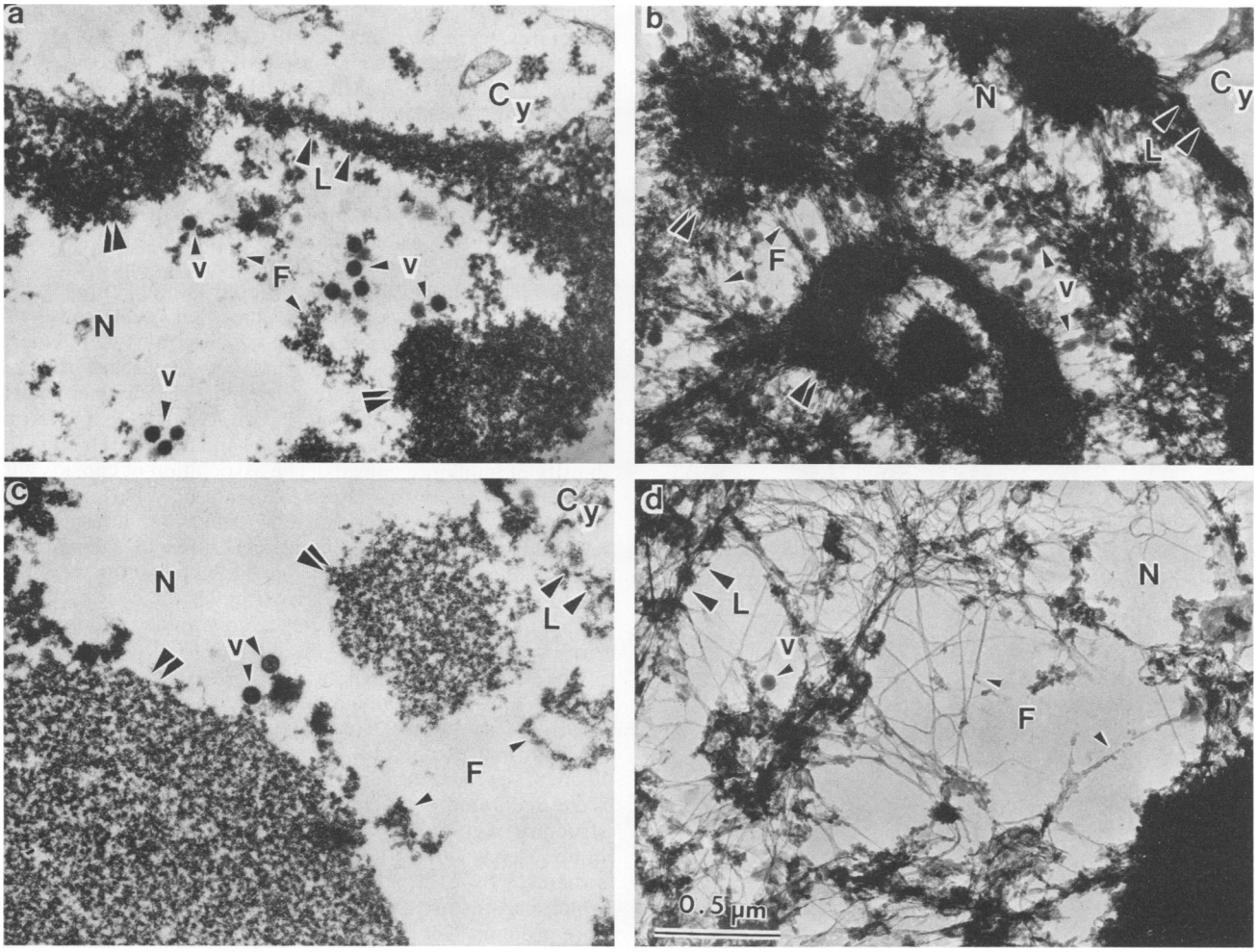

FIG. 1. Morphology of adenovirus-infected cells as revealed by Epon section and embedment-free techniques. These are views of HeLa cells after 28 h of adenovirus infection shown at a magnification of ×34,200. (a) Epon section of a cytoskeletal preparation. (b) Embedment-free section of a cytoskeletal preparation. (c) Epon section of an RNP-containing nuclear matrix preparation. (d) Embedment-free section of an RNP-containing nuclear matrix preparation. Symbols: N, nucleus; L, nuclear lamina; C_y, cytoplasmic region; F, filament of the nuclear matrix; double arrowheads, virus center; v, viral capsids. All micrographs show the interior of the infected cell nucleus. Viral capsids are imaged by both techniques, but the connections between capsids and the filaments of the nuclear matrix are seen best in embedment-free sections. In Epon sections, these filaments are rarely seen except in cross-section and the spatial relationships between viral capsids, viral centers, and the nuclear matrix are not easily visualized.

crenulations of the nuclear lamina. This has been observed in Epon-embedded sections by Lenk et al. (21), who proposed that nucleus-cytoplasm interactions are altered after infection. Some evidence for this could be seen in the cytoplasm surrounding the nucleus (Fig. 3c). The electron density of this area was lower than that of the peripheral cytoplasm, creating a halolike corona around the nucleus. This rearrangement of the cytoskeleton around the nucleus may be related to the laminar crenulation, since the intermediate filaments are anchored in the nuclear lamina (15). Compared with the 6-h infected cell (Fig. 3a and b), the chromatin was more condensed onto the nucleoli at 13 h and electron-dense areas, which may be virus-specific organizing centers, had appeared throughout the nucleus. Many of these structures were DNase I resistant (Fig. 3d) and were connected by the filaments of the nuclear matrix to each other and to the nuclear lamina. Many of the large electron-dense structures which at 6 h looked like modified nucleoli were granulated by this stage of infection, while a few remained amorphous or uniformly electron dense (Fig. 3d). The progression of morphological changes through infection suggests that nucleoli may be at the locations around which virus-related inclusions become organized.

At 28 h after infection (Fig. 3e and f), virus-related structures were prominent throughout the nucleus. Chromatin was very condensed, making it easier to see the nuclear matrix filaments that connected the many viral structures. Some of these structures are granulated, and some are uniformly electron dense. After DNase I treatment (Fig. 3f), areas within some of the granulated structures that may be fibrillar are visible.

High-magnification views of the adenovirus-infected HeLa cells (Fig. 4 to 6) showed in much greater detail the structural rearrangements accompanying infection. At 6 h after infection (Fig. 4), the cytoplasm of infected cells contained flattened vesicles associated with the meshwork of cytoplasmic fibers. These structures were not present in control cells, and in infected cells, they were present in

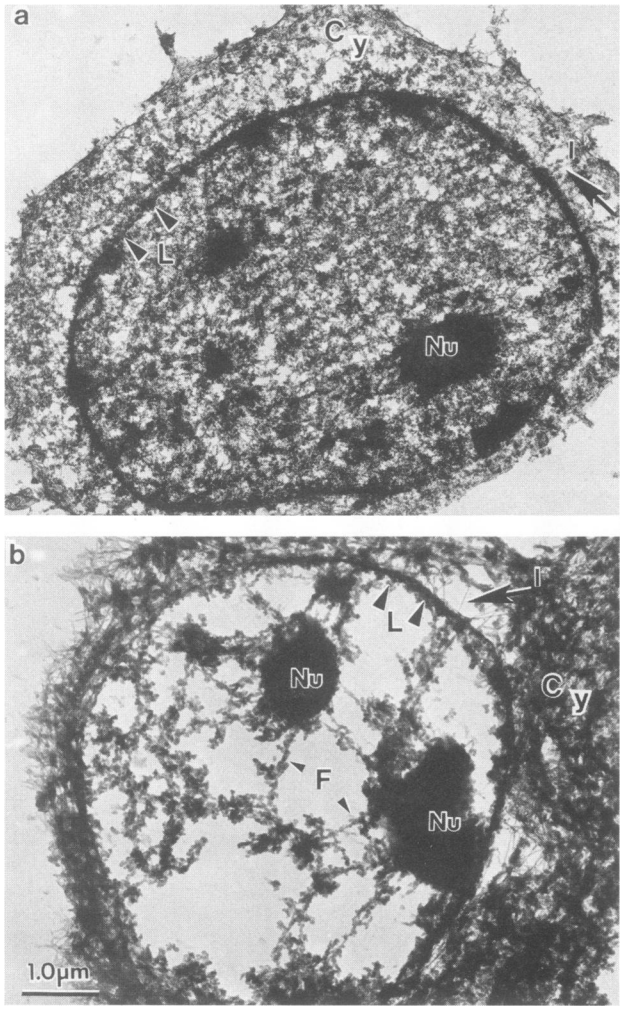

FIG. 2. Cytoskeleton and nuclear matrix of uninfected HeLa cells. These micrographs, shown at a magnification of ×10,200, are of embedment-free sections of control, mock-infected HeLa cells. (a) Cytoskeleton preparation. (b) RNP-containing nuclear matrix preparation. Symbols: Nu, nucleolus; L, nuclear lamina; C_y, cytoplasmic region; F, filaments of the nuclear matrix; I, intermediate filament. These are control views of the nuclear matrix and should be referred to for comparison when viewing pictures of infected cells. The nuclear lamina and nucleoli are easily visible. Intermediate filaments in the cytoplasmic region connect to the nuclear lamina. DNase I digestion removes chromatin, making the filaments of the nuclear matrix easier to see.

decreased numbers by 13 h and were not seen by 28 h. Occasionally, viral capsids were seen in the cytoplasm. These had the electron density of complete virions and not of empty capsids, and so they may be virions which had unproductively infected these cells. Aggregates of polyribosomes were present in the cytoplasmic region, enmeshed in the filaments of the cytoskeleton.

High-magnification views of 13-h-infected cells (Fig. 5) show the crenulated nuclear lamina in good detail. In many cells there appeared buds of lamina protruding from extruded sections of the lamina. Occasionally, these may have completely detached from the nucleus, existing as cytoplasmic structures or blebs (Fig. 5a), although we cannot exclude the possibility that they were connected to the lamina at a point outside this section. Electron-dense virus-related structures were seen in the nucleus in both granular and amorphous forms. After DNase I digestion (Fig. 5b), these structures could be clearly seen to be connected to each other by nuclear filaments which had become thickened and which were decorated with occasional viral capsids. These immature capsids had a lower electron density than did the mature virions seen later in infection. We believe these were empty capsid shells without DNA or the core proteins.

Many mature virions were seen in the nuclei of 28-h infected HeLa cells (Fig. 6). Each nucleus had been transformed into a large virus factory consisting of three distinguishable types of structure: amorphous electron-dense structures, granular regions from which virions were emerging, and filamentous attachments between these regions, attaching them to the nuclear lamina. The nuclear matrix filaments were decorated with two types of capsid, one having the density of mature virions and the other having the density of immature capsids. The association of capsids with filaments suggests that these filaments may be involved in transporting virions and various packaging intermediates between different virus-related structures in the nucleus. The attachments of viral capsids and the filaments were best seen in high-magnification views (Fig. 6b and c), which most clearly showed virions emerging from granular regions of the virus-organizing regions of the nucleus.

The three-dimensional arrangement of virus-organizing centers and their connecting filaments can be seen most clearly in stereo electron micrographs. Figure 7 presents such an image of HeLa cells after 28 h of infection. The filaments connecting amorphous and granular virus centers were decorated with capsids and mature virions. The fine structure of granular virus-related structures was seen better in this stereo view. Viral capsids could be seen within these structures by 28 h, suggesting that these are the regions in which capsids are assembled from capsomeres, DNA, and core proteins. The higher electron density of the amorphous regions makes both their internal structure and their possible function more obscure.

Infected HeLa cells had been lysed by 48 h after infection (Fig. 8). Remnants of the nuclear virus-related structures remained, and many virions were still attached to the residual nuclear matrix filaments. Release of virions took place slowly after cell lysis. Virions could be seen in the cytoplasmic regions as well as in the nuclear regions of these lysed cells, where some appeared to be attached to intermediate filaments.

DISCUSSION

Viral metabolism—transcription, translation, DNA replication, and viral assembly—does not take place in the soluble phase but rather occurs in association with the structural elements of the cell (reviewed in references 22 and 27). Many examples of this association of viral metabolism with cell architecture exist. The RNA metabolism of poliovirus (40) and simian virus 40 (1) occurs in association with the cytoskeletal framework. Virus-encoded polypeptides are associated with the cytoskeleton for both vesicular stomatitis virus (40) and herpes simplex virus (2). The herpes virus structural proteins are initially cytoskeletal but then enter the nucleus, where they are assembled into capsids on the nuclear matrix (2, 6, 14). The vesicular stomatitis virus nucleocapsid (9) and the poliovirus nucleocapsid (40) are assembled on the cytoskeleton.

Adenovirus is a nuclear virus; its transcription, DNA replication, and assembly occur in the nucleus (reviewed in

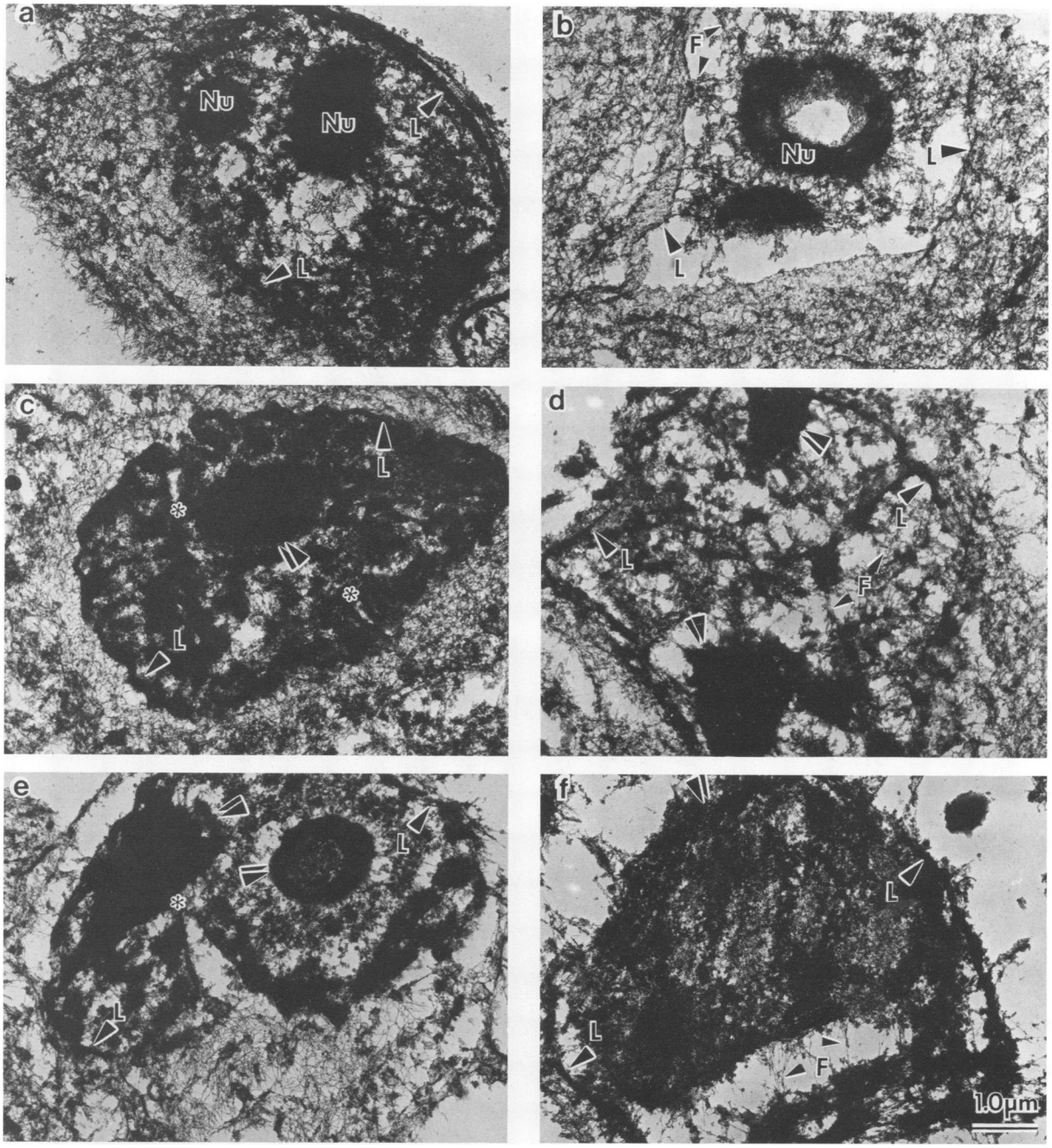

FIG. 3. Morphological changes at different times after adenovirus infection. This figure shows a time course of adenovirus-induced morphological changes, all shown at a magnification of ×9,300. (a, c, and e) Cytoskeletal preparations. (b, d, and f) RNP-containing nuclear matrix preparations. Symbols: Nu, nucleolus; L, nuclear lamina; F, filament of the nuclear matrix; double arrow heads, virus center; *, indentation in the nuclear lamina. (a and b) At 6 h after infection, the nucleus had moved to the periphery of the cell. This is more characteristic of infected cells. Chromatin was becoming condensed around the nucleoli and around the nuclear lamina. (c and d) By 13 h after infection, the nuclear lamina had become crenulated, changing the shape of the nucleus. Some of the indentations in the nuclear lamina (*) formed pinched-off pockets of cytoplasmic material in the nucleus. Large, electron-dense, DNase-resistant structures are visible in the nucleus. These might be either residual nucleoli or virus centers. There is a corona of decreased electron density around the nucleus, reflecting a rearrangement of intermediate filaments in that region. After DNase I digestion (panel d), the crenulations are not seen. Nuclear matrix filaments are aggregated around virus centers and link these centers together and to the nuclear lamina. (e and f) By 28 h after infection, the nucleus had become one large virus center consisting of uniformly electron-dense regions and granulated regions connected by the filaments of the nuclear matrix to each other and to the nuclear lamina. Some of the crenulations in the nuclear lamina had become extreme evaginations (*). Again, these cannot be seen after DNase I digestion (panel f). The cytoplasm around the nucleus has regions with few intermediate filaments (panel e).

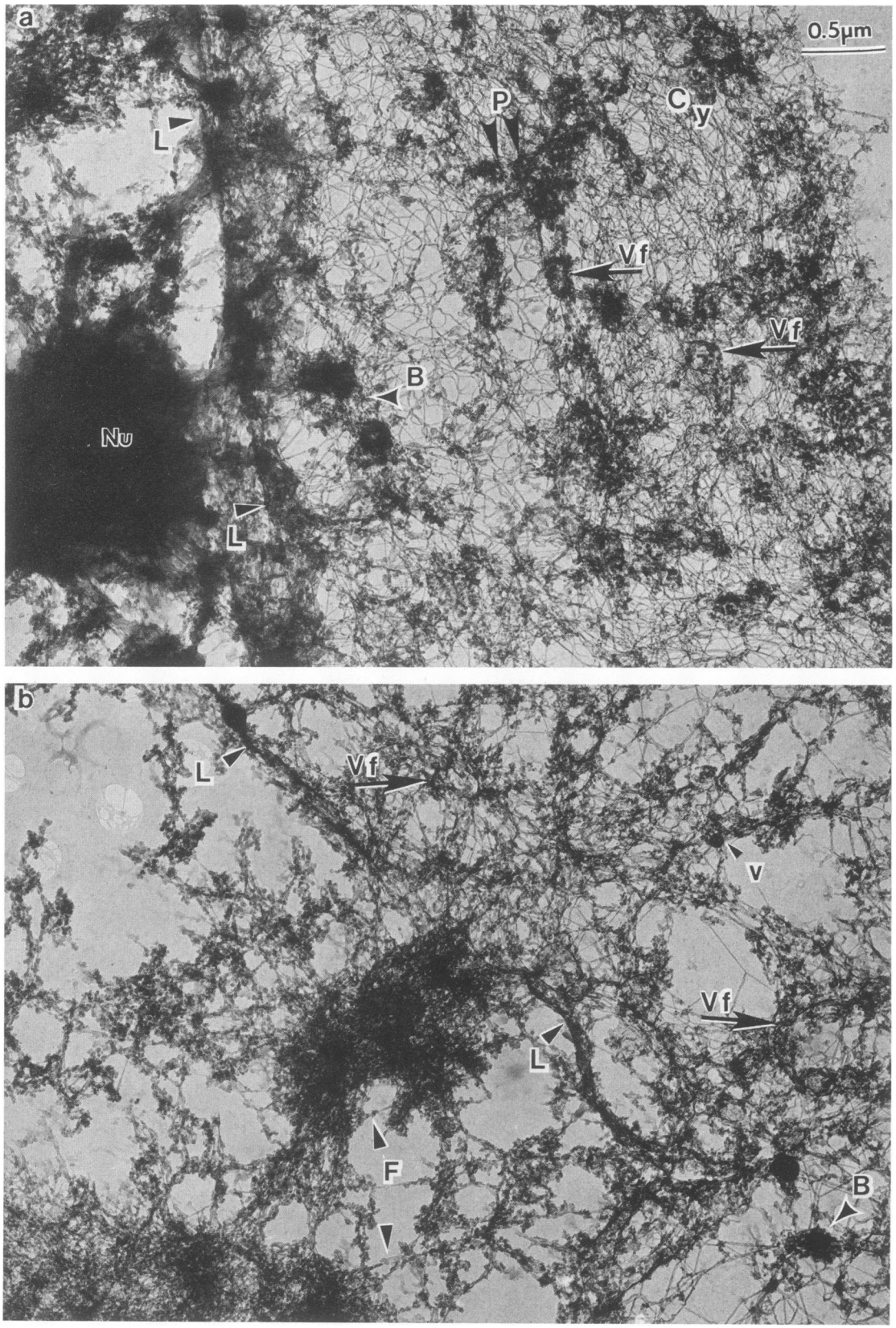

FIG. 4. Adenovirus-infected cells at 6 h after infection. This is a higher-magnification micrograph (×27,000) than in Fig. 3 and shows the filaments of the nuclear matrix and cytoskeleton in greater detail. (a) Cytoskeletal preparation. (b) RNP-containing nuclear matrix preparation. Symbols: Nu, nucleolus; L, nuclear lamina; C_y, cytoplasmic region; P, polyribosomes; B, electron-dense cytoplasmic bodies; F, filament of the nuclear matrix; v, virion; Vf, flattened vesicle. In panel a, the nucleolus is close to the nuclear lamina and seems to have chromatin condensed around it and is surrounded by areas free of chromatin. Aggregated polyribosomes are enmeshed in the network of intermediate filaments, which also entrap electron-dense bodies (marked by B). After DNase I digestion (panel b), chromatin was removed, revealing in greater detail the filaments of the nuclear matrix. A flattened vesicle can be seen in the cytoplasmic region, as well as a virion which may have unproductively infected this cell.

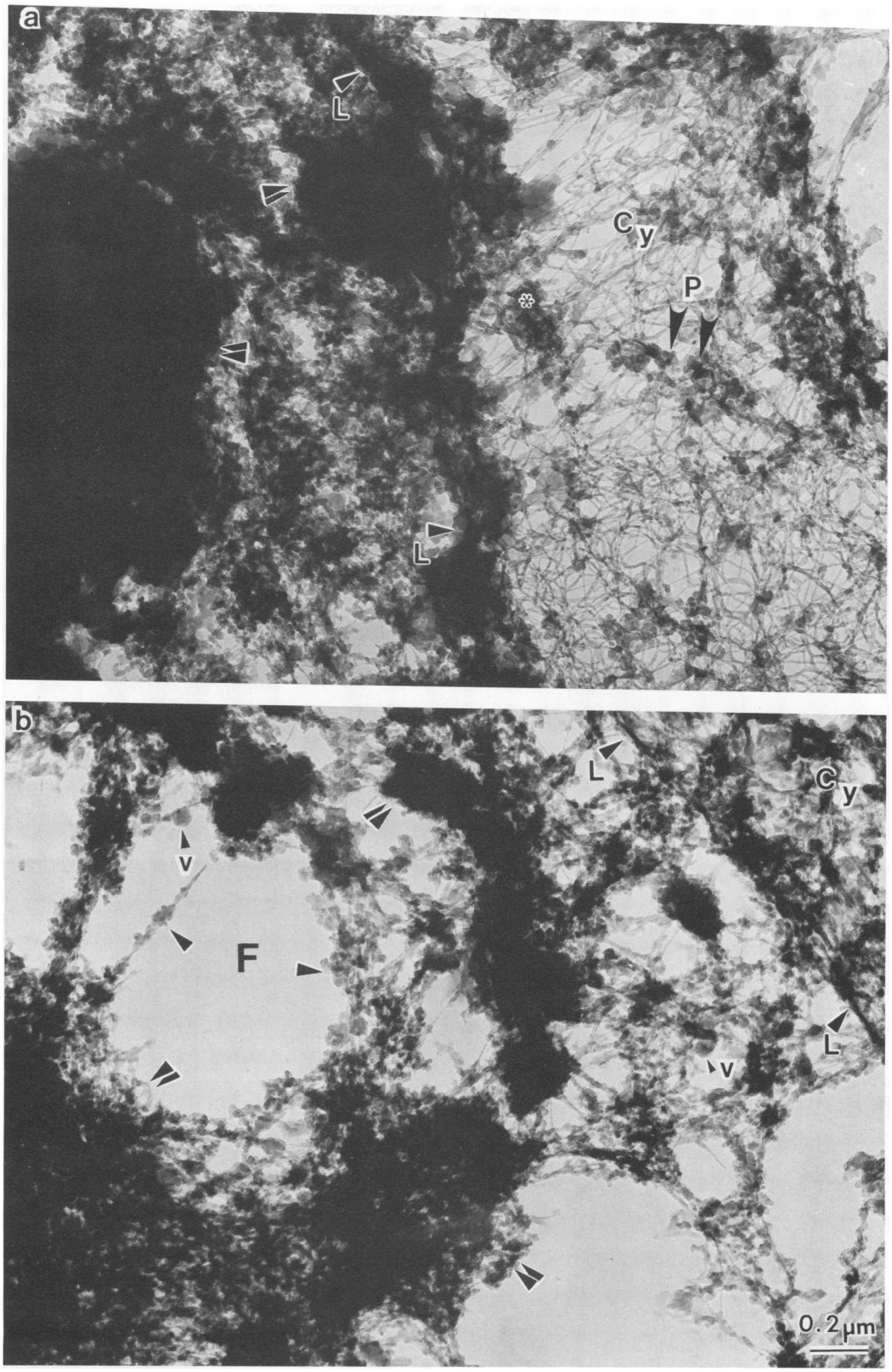

FIG. 5. Adenovirus-infected cells at 13 h after infection. These micrographs are presented at a magnification of ×45,000. (a) Cytoskeleton preparation. (b) RNP-nuclear matrix preparation. Symbols: L, nuclear lamina; C_y, cytoplasmic region; F, filament of the nuclear matrix; double arrowheads, virus center in the nucleus; v, viral capsid; P, aggregated polyribosomes; *, blebs of nuclear material in the cytoplasm. Aggregates of polyribosomes can still be seen enmeshed in the intermediate filaments. The nuclear lamina in panel a is crenulated and has condensed chromatin along its nuclear surface. Material with the density of nuclear material is budding from the nuclear lamina and may pinch off completely, forming nuclear blebs (*) in the cytoplasm. After DNase I digestion, chromatin was removed, and within the nucleus, virus centers consisting of both amorphously electron-dense and granulated regions are seen connected to each other and to the lamina by filaments of the nuclear matrix. Viral capsids can be seen emerging from regions of the virus centers. These are less electron dense than mature virions and may therefore be empty capsids.

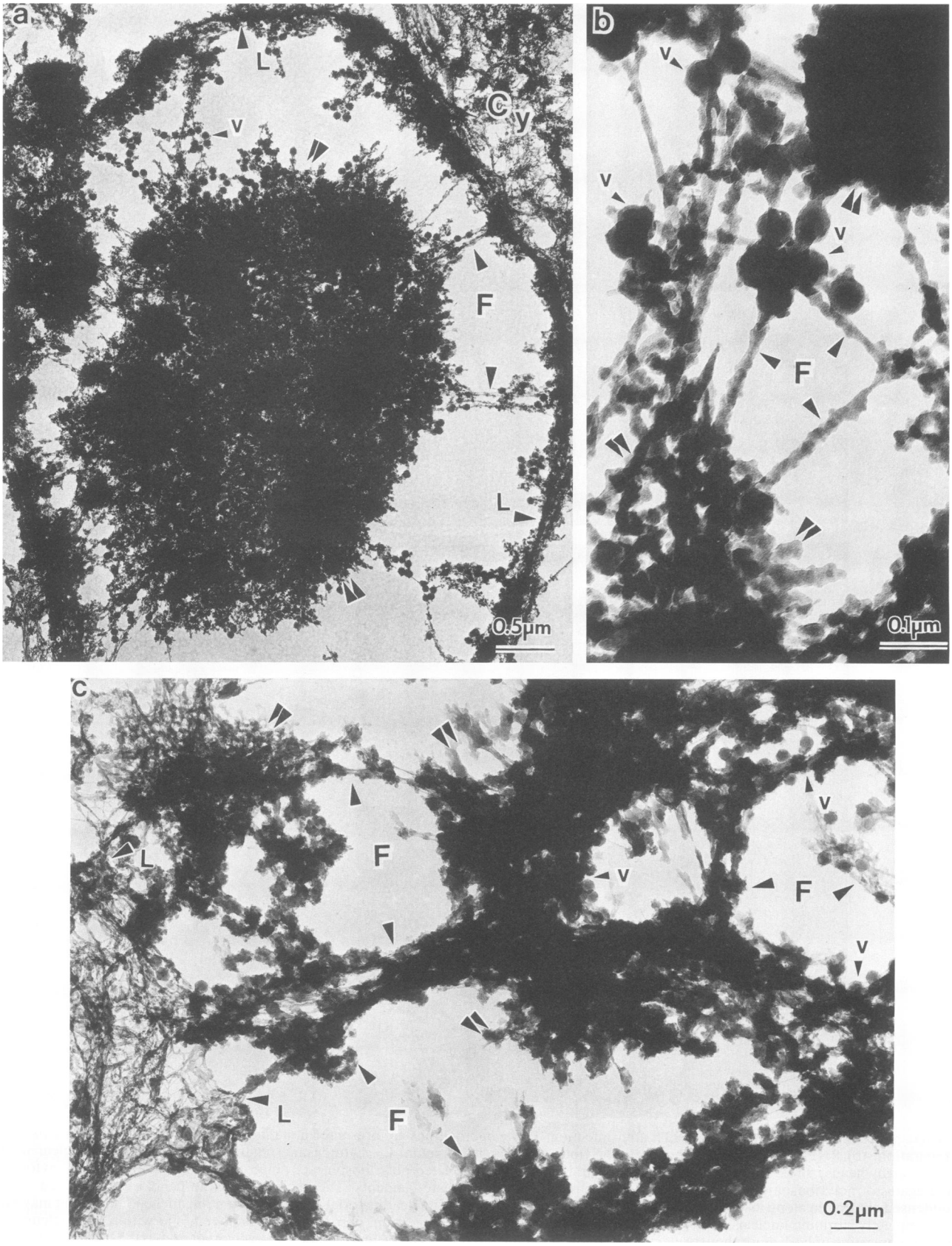
a
L
V
Cy
F
L
0.5μm
b
V
V
V
F
0.1μm
c
L
F
V
V
F
V
L
F
0.2μm

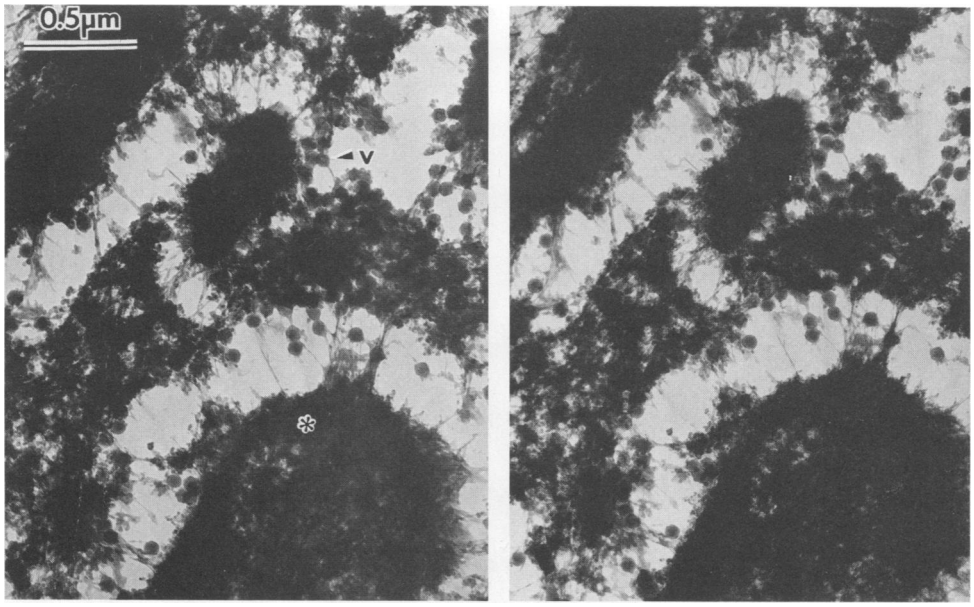

FIG. 7. Stereo micrograph of an infected cell at 28 h after infection. This view of a cytoskeletal preparation is shown at a magnification of ×30,000 and shows only the nuclear region of the cell. Viral capsids (v) are bound to the nuclear matrix filaments which connect regions of the virus center to each other and to the nuclear lamina. The granulated regions of the virus centers are revealed in greater detail in stereo. Many granulations are the size of (75 nm) and are seen to be viral capsids. These granulated regions may be regions of capsid assembly or virion storage. A viral capsid (*) can be seen enmeshed in the central virus center. The details in this micrograph can be best seen with the use of a standard stereo viewer.

reference 19). It would seem likely, therefore, that adenovirus metabolism occurs in association with the underlying structural elements of the nucleus, the nuclear matrix. In fact, transcription of adenovirus sequences and their splicing into mature mRNA is known to occur on the nuclear matrix (23), and adenovirus early region proteins have been found bound to the nuclear matrix (13, 36), where they may be involved in regulation of viral transcription.

Traditional Epon embedment section electron microscopy is a very good technique for showing many features of cell morphology. This technique preserves cell organelles and provides a good view of membrane systems and the connections between them. It would be the ideal technique for studying, for example, the changes in smooth endoplasmic reticulum that follow adenovirus infection (21). Unfortunately, the use of stained Epon-embedded sections is not ideal for studying the cytoskeleton or nuclear matrix of cells. For example, the filaments of the nuclear matrix, which connect virus-related structures and the nuclear lamina, are seen only in cross-section (Fig. 1) unless they are both close to and parallel to the surface of the section, something which occurs rarely. Thus, a different technique is required for the study of adenovirus interactions with the cytoskeleton or nuclear matrix. A set of extraction and sectioning techniques which are ideal for studying the filamentous skeletons of the cell and which have been used in this study to examine adenovirus-specific rearrangements of the nuclear matrix have been developed in this laboratory (7, 15). These techniques involve the use of embedment-free section electron microscopic procedures similar to those pioneered by Wolosowick (43).

The extraction technique used in this study has several steps (15). In the first step, the plasma membrane lipids are removed and the soluble components of the cell diffuse away in 0.5% Triton X-100, leaving an extensive cytoskeletal framework and nucleus. In some cases, cells are fixed, sectioned, and examined after this step. In others, the cytoskeleton is then stripped by extraction with double detergent in RSB. This step leaves demembranated, chromatin-containing nuclei with attached and radiating intermediate filaments. The chromatin is removed by digestion in DNase I followed by extraction with 0.25 M ammonium sulfate. The resulting RNP-containing nuclear matrix-intermediate filament preparation is then fixed, sectioned, and examined.

Extracted cells are prepared for electron microscopy by

FIG. 6. Adenovirus-infected cells at 28 h after infection. These are higher-magnification micrographs of the cytoskeleton and nuclear matrix than were presented in Fig. 3. Symbols: L, nuclear lamina; C_y, cytoplasmic region; F, filament of the nuclear matrix; double arrowheads, virus center in the nucleus; v, viral capsids. (a) This micrograph of a cytoskeleton preparation, shown at a magnification of ×22,000, reveals a large virus center in the center of the nucleus connected by filaments of the nuclear matrix to the nuclear lamina. Mature virions can be seen emerging from this structure, and they decorate the nuclear matrix fibers. The large virus-specific structure of virus center consists of both amorphous dense regions and granulated regions. (b) This micrograph shows a similar cytoskeleton preparation at a higher magnification (×120,000). We can see the intimate contact between the filaments of the nuclear matrix and virions and the anchoring of those filaments in the corner of a viral center from which virions appear to be emerging. (c) This micrograph shows the interior of the nucleus in an RNP-nuclear matrix preparation at a magnification of ×41,000. Filaments of the nuclear matrix can be seen connecting the DNase I-resistant virus center to the nuclear lamina, which is cut in a tangential way in this section. These filaments are beginning to bundle, and virus centers are beginning to overlap onto the filaments. Virions decorate these filaments, especially in the vicinity of the virus center.

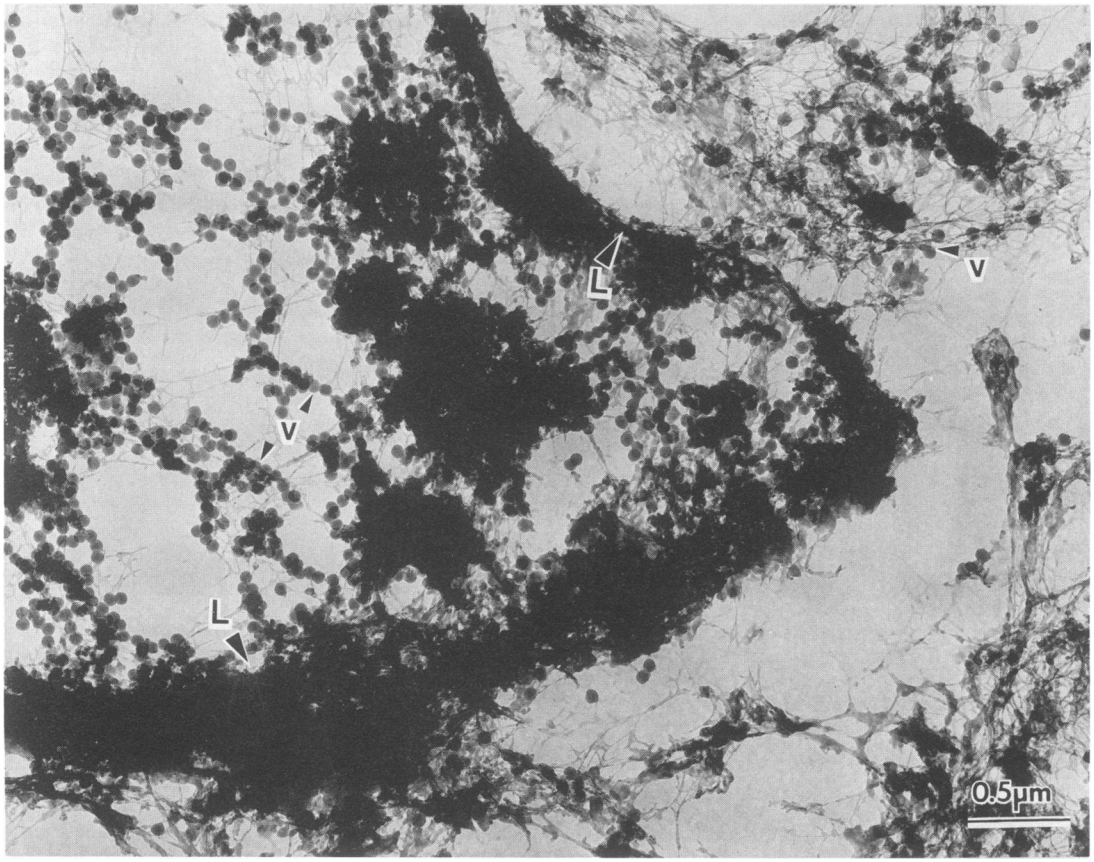

FIG. 8. Lysed cell at 44 h after infection. This micrograph shows a cytoskeletal preparation of a lysed cell at a magnification of ×27,000. Many virions (v) are attached to the remnants of the nuclear matrix filaments in the nucleus and to intermediate filaments in the cytoplasmic region which are connected to the nuclear lamina (L).

fixation in glutaraldehyde and embedment in diethylene glycol distearate. After sectioning, the diethylene glycol distearate embedding resin is removed by solvent extraction. The section is viewed without staining of any type. The filaments of the cytoskeleton and nuclear matrix can be easily seen without staining in the absence of embedding material. The lack of embedding resin allows us to see the interior of the section and not just the surface.

These techniques provide a unique window to the progressive adenovirus-caused rearrangements of the nuclear matrix following infection. Rearrangement of the nuclear matrix was evident as early as 6 h after infection and continued progressively until the nucleus had become one large virus factory that produced virions and stored them until cell lysis.

At 6 h after infection, chromatin was seen collapsing around nucleoli to form large electron-dense structures which were larger than the nucleoli of control cells. It appears to us that these altered nucleoli mark the focus around which the nuclear matrix is rearranged into virus-related structures. It is difficult to determine exactly when a nucleolus has become a virus center. Certainly, at later stages of infection, when viral capsids can be seen in these structures, they are virus centers. It will be interesting to determine in future studies whether nucleolar material is retained within these structures late in infection.

As infection progressed to 13 h, there was further condensation of chromatin onto these amorphously electron-dense centers and there appeared smaller electron-dense structures in the nucleus which were connected to each other, to the larger centers, and to the nuclear lamina by the fibers of the nuclear matrix. By 28 h, many granulated areas had appeared in the nuclear matrix. In high-magnification views, these could be seen to contain viral capsids of about 75 nm in diameter. More capsids could be seen emerging from these granulated structures and bound to the nuclear matrix fibers that hold these structures together and anchor them to the nuclear lamina.

We propose that virus-related structures of the nuclear matrix are composed of at least three areas which we see by electron microscopy as (i) amorphously electron-dense regions with capsid sized granulations on their periphery, (ii) granulated regions whose granulations are composed of viral capsids, and (iii) filaments which connect these structures to each other and anchor them to the lamina. The decoration of filaments with capsids suggests that they may be involved in the transport of capsids and capsid intermediates between the other structures. The granulated regions contain capsids, and we propose that they are regions of capsid assembly and storage. Amorphous regions have the electron density of DNA and may be the sites of viral DNA replication. The apparent emergence of capsid-sized granulations from their periphery suggests to us that DNA is packaged into empty capsid cores at this location.

There are two distinguishable types of viral capsid, both of the same size but differing in their electron density. The most likely explanation for this is that the less electron-dense capsids represent the immature capsids that have been constructed from capsomeres, while the more electron-

dense capsids are more mature forms having viral genomic DNA and the core proteins packaged within them. At 13 and 28 h, there are also microparticles of about 11 nm in diameter associated with the nuclear matrix fibers and seen only in high-magnification micrographs (not shown). These may represent the capsomeres from which empty viral capsids are assembled.

The nuclear lamina changes dramatically between 6 and 13 h of infection, becoming crenulated. This phenomenon has been observed in conventional Epon-embedded sections by Lenk et al. (21), who found points at which the nuclear envelope folded back on itself, forming a trilaminar configuration. They suggested that these regions sometimes bud off to form nuclear vesicles or blebs in the cytoplasm. Such blebs can be seen in Fig. 4. These nuclear pieces have the density of condensed chromatin and may contain chromatin which first collapsed onto the lamina. Lenk et al. (21) proposed that these changes in the nuclear lamina were evidence of altered nucleus-cytoplasm interactions. We can see other evidence of changes at the nucleus-cytoplasm boundary. The cytoskeleton in the perinuclear region of the cytoplasm has decreased in fiber density by 13 h after infection (Fig. 3c), producing a halolike effect around the nucleus. The real significance of nuclear lamina and perinuclear cytoplasmic changes can only be speculated about and requires much further study.

The use of gentle, progressive extraction techniques and of embedment-free section electron microscopy provides a new view of the rearrangements in nuclear structure that accompany adenovirus infection. The combination of these techniques with immuno-gold staining for specific adenovirus proteins and with in situ hybridization of adenoviral nucleic acid sequences should facilitate the more complete understanding of adenovirus metabolism and assembly.

ACKNOWLEDGMENTS

Jeffrey A. Nickerson is the recipient of a Postdoctoral Fellowship from the Cancer Research Institute.

We thank Phillip A. Sharp for his gift of adenovirus.

LITERATURE CITED

1. **Ben-Ze'ev, A., R. Abulafia, and Y. Aloni.** 1982. SV40 virions and viral RNA metabolism are associated with cellular substructures. EMBO J. **1**:1225–1231.
2. **Ben-Ze'ev, A., R. Abulafia, and S. Bratosin.** 1983. Herpes simplex virus and protein transport are associated with the cytoskeletal framework and the nuclear matrix in infected BSC-1 cells. Virology **129**:501–507.
3. **Berezney, R., and L. A. Buchholtz.** 1981. Dynamic association of replicating DNA fragments with the nuclear matrix of regenerating liver. Exp. Cell Res. **132**:1–13.
4. **Berezney, R., and D. S. Coffey.** 1974. Identification of a nuclear protein matrix. Biochem. Biophys. Res. Comun. **60**:1410–1417.
5. **Berezney, R., and D. S. Coffey.** 1975. Nuclear protein matrix: association with newly synthesized DNA. Science **189**:291–292.
6. **Bibor-Hardy, V., M. Pouchelet, E. St. Pierre, M. Herzberg, and R. Simard.** 1982. The nuclear matrix is involved in herpes simplex virogenesis. Virology **121**:296–306.
7. **Capco, D. G., G. Krochmalnic, and S. Penman.** 1984. A new method for preparing embedment-free sections for transmission electron microscopy: applications to the cytoskeletal framework and other three-dimensional networks. J. Cell Biol. **98**:1878–1885.
8. **Capco, D. G., K. M. Wan, and S. Penman.** 1982. The nuclear matrix: three-dimensional architecture and protein composition. Cell **29**:847–858.
9. **Chatterjee, P. K., M. M. Cervera, and S. Penman.** 1984. Formation of vesicular stomatitis virus nucleocapsid from cytoskeletal framework-bound N protein: possible model for structure assembly. Mol. Cell. Biol. **4**:2231–2234.
10. **Ciejek, E. M., M.-J. Tsai, and B. W. O'Malley.** 1983. Actively transcribed genes are associated with the nuclear matrix. Nature (London) **306**:607–609.
11. **D'Halluin, J. C., G. R. Martin, G. Torpier, and P. A. Boulanger.** 1978. Adenovirus type 2 assembly analyzed by reversible cross-linking of labile intermediates. J. Virol. **26**:357–363.
12. **D'Halluin, J. C., M. Milleville, P. A. Boulanger, and G. R. Martin.** 1978. Temperature-sensitive mutant of adenovirus type 2 blocked in virion assembly: accumulation of light intermediate particles. J. Virol. **26**:344–356.
13. **Feldman, L. T., and J. R. Nevins.** 1983. Location of the adenovirus E1a protein, a positive acting transcriptional factor, in infected cells. Mol. Cell. Biol. **3**:829–838.
14. **Fenwick, M. L., M. J. Walker, and J. Petkevich.** 1978. On the association of virus proteins with the nuclei of cells infected with herpes simplex virus. J. Gen. Virol. **39**:519–529.
15. **Fey, E. G., G. Krochmalnic, and S. Penman.** 1986. The nonchromatin substructures of the nucleus: the ribonucleoprotein (RNP)-containing and RNP-depleted matrices analyzed by sequential fractionation and resinless section electron microscopy. J. Cell Biol. **102**:1654–1665.
16. **Fisher, P. A., M. Berrios, and G. Blobel.** 1982. Isolation and characterization of a proteinaceous subnuclear fraction composed of nuclear matrix, peripheral lamina and nuclear pore complexes from embryos of *Drosophila melanogaster*. J. Cell Biol. **92**:674–686.
17. **Hentzen, P. C., J. H. Rho, and I. Bekhor.** 1984. Nuclear matrix DNA from chicken erythrocytes contains β-globin gene sequences. Proc. Natl. Acad. Sci. USA **81**:304–307.
18. **Horne, R. W., S. Bonner, A. P. Waterson, and P. Wildy.** 1959. The icosohedral form of an adenovirus. J. Mol. Biol. **1**:84–86.
19. **Horwitz, M. S.** 1985. Adenoviruses and their replication, p. 433–476. *In* B. N. Fields (ed.), Virology. Raven Press, New York.
20. **Horwitz, M. S., M. D. Scharff, and J. V. Maizel, Jr.** 1969. Synthesis and assembly of adenovirus 2. I. Polypeptide synthesis, assembly of capsomeres, and the morphogenesis of the virion. Virology **39**:682–684.
21. **Lenk, R., T. Storch, and J. V. Maizel, Jr.** 1980. Cell architecture during adenovirus infection. Virology **105**:19–34.
22. **Luftig, R. B.** 1982. Does the cytoskeleton play a significant role in animal virus replication? J. Theor. Biol. **99**:173–191.
23. **Mariman, E. C. M., C. A. G. van Eekelen, R. J. Reinders, A. J. M. Berns, and W. J. van Venrooij.** 1982. Adenoviral heterogeneous nuclear RNA is associated with the host nuclear matrix during splicing. J. Mol. Biol. **154**:103–119.
24. **McCready, S. J., J. Godwin, D. W. Mason, I. A. Brazell, and P. R. Cook.** 1980. DNA is replicated at the nuclear cage. J. Cell Sci. **46**:365–386.
25. **Mirkovitch, J., M.-E. Mirault, and U. K. Laemmli.** 1984. Organization of the higher-order chromatin loop: specific DNA attachment sites on nuclear scaffold. Cell **39**:223–232.
26. **Pardoll, D. M., B. Vogelstein, and D. S. Coffey.** 1980. A fixed site of DNA replication in eukaryotic cells. Cell **19**:527–536.
27. **Penman, S.** 1985. Virus metabolism and cellular architecture, p. 169–182. *In* B. N. Fields (ed.), Virology. Raven Press, New York.
28. **Pereira, H. G.** 1958. A protein factor responsible for the early cytopathic effect of adenoviruses. Virology **6**:601–611.
29. **Petterson, U., L. Philipson, and S. Hoglund.** 1967. Structural proteins of adenovirus. I. Purification and characterization of the adenovirus type 2 hexon antigen. Virology **33**:575–590.
30. **Phillips, D. M., and H. J. Raskas.** 1972. Ultrastructural changes in KB cultures infected with adenovirus type 2. Virology **48**:156–169.
31. **Prage, L., S. Hoglund, and L. Philipson.** 1972. Structural proteins of adenovirus. VIII. Characterization of incomplete particles of adenovirus type 3. Virology **49**:745–757.
32. **Precious, B., and W. C. Russell.** 1985. Growth, purification, and titration of adenoviruses, p. 193–205. *In* B. W. J. Mahy (ed.), Virology: a practical approach. IRL Press, Oxford.

33. **Reynolds, E. S.** 1963. The use of lead citrate at high pH as an electron-opaque stain in electron microscopy. J. Cell Biol. **17**:208–213.
34. **Robinson, S. I., B. D. Nelkin, and B. Vogelstein.** 1982. The ovalbumin gene is associated with the nuclear matrix of chicken oviduct cells. Cell **28**:99–106.
35. **Ross, D. A., R. W. Yen, and C. B. Chae.** 1982. Association of globin ribonucleic acid and its precursors with the chicken erythroblast nuclear matrix. Biochemistry **21**:764–771.
36. **Sarnow, P., P. Hearing, C. W. Anderson, N. Reich, and A. J. Levine.** 1982. Identification and characterization of an immunologically conserved adenovirus early region 11,000 Mr protein and its association with the nuclear matrix. J. Mol. Biol. **162**:565–583.
37. **Schrom, M., and R. Bablanian.** 1981. Altered cellular morphology resulting from cytocidal virus infection. Arch. Virol. **70**:173–187.
38. **Small, D., B. Nelkin, and B. Vogelstein.** 1985. The association of transcribed genes with the nuclear matrix of *Drosophila* cells during heat shock. Nucleic Acids Res. **13**:2413–2431.
39. **Smith, H. C., R. Berezney, J. M. Brewster, and D. Rekosh.** 1985. Properties of adenoviral DNA bound to the nuclear matrix. Biochemistry **24**:1197–1202.
40. **Weed, H. G., G. Krochmalnic, and S. Penman.** 1985. Poliovirus metabolism and the cytoskeleton framework: detergent extraction and resinless section electron microscopy. J. Virol. **56**:549–557.
41. **Wilchek, M., and M. Gorecki.** 1969. Affinity chromatography of bovine pancreatic ribonuclease A. Eur. J. Biochem. **11**:491–494.
42. **Wold, S. M., M. Green, and W. Buttner.** 1978. Adenoviruses, p. 673–678. *In* D. P. Nyack (ed.), The molecular biology of animal viruses. Marcel Dekker, Inc., New York.
43. **Wolosewick, J.** 1980. The application of polyethylene glycol (PEG) to electron microscopy. J. Cell Biol. **86**:675–681.
44. **Younghusband, H. B., and K. Maundrell.** 1982. Adenovirus DNA is associated with the nuclear matrix of infected cells. J. Virol. **43**:705–713.